



HAL
open science

AMPA receptor activation controls type I metabotropic glutamate receptor signalling via a tyrosine kinase at parallel fibre-Purkinje cell synapses

Céline Auger, David Ogden

► **To cite this version:**

Céline Auger, David Ogden. AMPA receptor activation controls type I metabotropic glutamate receptor signalling via a tyrosine kinase at parallel fibre-Purkinje cell synapses. *The Journal of Physiology*, 2010, 588 (16), pp.3063 - 3074. 10.1113/jphysiol.2010.191080 . hal-03458012

HAL Id: hal-03458012

<https://hal.science/hal-03458012>

Submitted on 12 Oct 2022

HAL is a multi-disciplinary open access archive for the deposit and dissemination of scientific research documents, whether they are published or not. The documents may come from teaching and research institutions in France or abroad, or from public or private research centers.

L'archive ouverte pluridisciplinaire **HAL**, est destinée au dépôt et à la diffusion de documents scientifiques de niveau recherche, publiés ou non, émanant des établissements d'enseignement et de recherche français ou étrangers, des laboratoires publics ou privés.

**AMPA receptor activation controls type I metabotropic
glutamate receptor signaling via a tyrosine kinase at parallel
fibre-Purkinje cell synapses.**

Abbreviated title: AMPAR regulation of mGluR1

Céline Auger and David Ogden.

Laboratoire de Physiologie cérébrale (UMR8118)

Université Paris Descartes

45, rue des Saints Pères

75006 PARIS FRANCE

Corresponding author:

Céline Auger

Laboratoire de Physiologie cérébrale, UMR8118

Université Paris Descartes

45, rue des Saints Pères, 75006 PARIS.

Tel: (33) 01 42 86 38 04

Fax: (33) 01 42 86 38 30

celine.auger@parisdescartes.fr

Keywords: mGluR1, AMPA receptors, cerebellum.

5998 words

Table of content category : Neuroscience.

Non-technical summary:

The metabotropic glutamate receptor type I is a G-protein linked receptor for the neurotransmitter L-glutamate with slow transduction kinetics. It is highly expressed in cerebellar Purkinje cells where it activates signaling pathways that influence excitability and intracellular Ca²⁺. It has been shown to be required for motor coordination and learning. We show in this study that metabotropic receptor signaling can be regulated by fast glutamate receptors following synaptic release of the neurotransmitter. This work enhances our understanding of the conditions required to activate and regulate signaling via these receptors.

Abstract:

Metabotropic glutamate receptors type I (mGluR1) and ionotropic AMPA receptors (AMPA) are colocalized at parallel fiber (PF) to Purkinje cell synapses of the cerebellum. Single stimulation of PFs activates fast AMPAR excitatory postsynaptic currents, whereas the activation of mGluR1 requires burst stimulation. mGluR1 signal through several pathways in Purkinje cells and the most prominent is the activation of a slow EPSC (sEPSC). To separate the two synaptic currents, studies of the sEPSC have commonly been performed in the presence of AMPA/KA receptor antagonists. We show here in rat cerebellar slices that inhibition of the fast EPSC by AMPAR antagonists strongly and selectively potentiates the mGluR1 sEPSC, showing a negative regulation of mGluR1 by AMPAR. This effect is observed with low concentrations of NBQX (300 nM to 1 μ M), with the selective AMPAR antagonist GYKI 53655 and also with γ -DGG, a low affinity glutamate receptor antagonist. When photorelease of glutamate from MNI-glutamate was used to study the postsynaptic responses in isolation, AMPAR inhibition produced a similar potentiation of the mGluR1 sEPSC, showing that the interaction is postsynaptic. Finally, perfusion of the postsynaptic cell with PP1, an inhibitor of src-family tyrosine kinase, increased

the amplitude of the mGluR1 sEPSC and occluded the effect of AMPAR inhibition. Thus, at PF to Purkinje cell synapses, AMPAR activation inhibits the mGluR1 sEPSC via activation of a src-family tyrosine kinase. Consequently mGluR1 signaling will be more sensitive to spillover of glutamate than to local synaptic release. Furthermore, it will be enhanced at silent PF synapses which are the majority in Purkinje cells.

Abbreviations

AMPA, AMPA receptor; D-AP5, D-(-)-2-Amino-5-phosphonopentanoic acid; bpv(Phen), Bisperoxo(1,10-phenanthroline)oxovanadate; 7-Cl-Kyn, 7-Chlorokinurenic acid; CNQX, 6-cyano-7-nitroquinoxaline-2,3-dione; CPCCOEt, 7-(Hydroxyiminocyclopropa[b]chromen-1a-carboxylate ethyl ester; γ -DGG, γ -D-Glutamylglycine; DNQX, 6,7-dinitroquinoxaline-2,3-dione; GYKI 53655, 1-(4-aminophenyl)-3-methylcarbonyl-4-methyl-7,8-methylenedioxy-3,4-dihydro-5H-2,3-benzodiazepine; KAR, Kainate receptor; LTD, long term depression; mGluR1, metabotropic glutamate receptor type I; MNI-glutamate, 4-methoxy-7-nitroindolyl-L-glutamate; NBQX, 2,3-Dioxo-6-nitro-1,2,3,4-tetrahydrobenzo[f]quinoxaline-7-sulfonamide; NPE-HPTS, 2-nitrophenylethyl ether of pyranine; PF, parallel fibre; PP1, 1-(1,1-Dimethylethyl)-1-(4-methylphenyl)-1H-pyrazolo[3,4-d]pyrimidin-4-amine; PTK, protein tyrosine kinase; sEPSC, slow EPSC; SR 95531, 2-(3-Carboxypropyl)-3-amino-6-(4methoxyphenyl)pyridazinium bromide.

Introduction

Fast ionotropic receptors of the AMPA/KA type and slow metabotropic glutamate receptors type 1 (mGluR1) coexist at parallel fiber (PF) to Purkinje cell synapses in the cerebellum. Single stimulation of PFs is sufficient to activate postsynaptic AMPARs, but activation of mGluR1 requires burst stimulation to produce sufficient accumulation of the neurotransmitter (Batchelor

et al., 1994) and the resulting sEPSC is strongly modulated by glutamate transporters (Brasnjo and Otis, 2001; Reichelt and Knopfel, 2002). mGluR1s are inserted at the periphery of excitatory synapses (Baude et al., 1993; Nusser et al., 1994; Petralia et al., 1998) where they can monitor glutamate released at the same synapse but also that diffusing from nearby synapses.

Activation of mGluR1 in cerebellar Purkinje cells triggers intracellular signalling pathways downstream of the G protein Gq (Hartmann et al., 2004). These pathways generate two electrophysiological signals: a sEPSC (Batchelor et al., 1994) and a K⁺ current mediated by BK channels activated by inositol trisphosphate evoked Ca²⁺ release (Canepari and Ogden, 2006). mGluR1 activation also stimulates the production of endocannabinoids (Galante and Diana, 2004; Maejima et al., 2005) and potentiates T-type Ca²⁺ channels (Hildebrand et al., 2009). Burst stimulation of PFs most commonly gives rise to the sEPSC. The underlying conductance change is due to non-selective cation channels permeable to Ca²⁺ (Canepari et al., 2001, 2004; Tempia et al., 2001), identified as TRPC3 (Hartmann et al., 2008), generating a slow rise of intracellular Ca²⁺ (Canepari et al., 2004; Canepari and Ogden, 2006). Coupling of the channel to mGluR1 is independent of PLC β (Hirono et al., 1998; Canepari et al., 2001; Tempia et al., 2001; Canepari and Ogden, 2006) and mGluR1 signaling is regulated by tyrosine phosphorylation (Canepari and Ogden, 2003, 2006; Hildebrandt et al., 2009).

Evidence from paired granule cell to Purkinje cell recording suggests that PF synapses are most often silent (Isopes and Barbour, 2002) and that the pattern and prevalence of silent synapses contributes to information storage (Brunel et al., 2004). A survey of studies of the sEPSC shows that in all reports experiments were made in the presence of AMPA receptor antagonists (CNQX, NBQX, DNQX or GYKI) a condition that artificially silences the synapse (Batchelor and Garthwaite, 1993, 1997; Brasnjo and Otis, 2001; Canepari et al., 2001, 2004; Tempia et al., 2001; Dzubay and Otis, 2002; Kim et al., 2003; Canepari and Ogden, 2003, 2006; Hartmann et al., 2004; Marcaggi and Attwell, 2005; Wadiche and Jahr, 2005; Jin et al., 2007, see single exception of Tempia

et al. (1998) Fig. 1). Although it is often argued that AMPAR antagonists were required simply to separate the fast and slow EPSCs, we have found evidence that they influence the functional expression of the mGluR1 pathway.

We show here that AMPAR inhibition enhances the mGluR1 sEPSC. Further, the contributions of pre and postsynaptic mechanisms were investigated by photolytic release of L-glutamate from MNI-caged glutamate and the possible coupling mechanisms between the fast and slow EPSCs were investigated pharmacologically. The results show a negative regulation of mGluR1 signalling by postsynaptic AMPAR activation and provide evidence for the involvement of tyrosine phosphorylation.

Material and Methods

Ethical approval: Sprague Dawley rats were provided by Janvier (St Berthevin, France) and subsequently housed at the central animal house at University Paris Descartes (centre St Pères, approval number A-750607), approved by the “Prefecture de Police” following inspection by Veterinary Services of the city of Paris, and representatives of the french ministry of research and the ministry for Health, in agreement with the European Directive 86/609/EEC regarding the protection of animals used for experimental and other scientific purposes.

Experimental procedures were approved by the Directorate of Paris Veterinary Services, by the scientific committee of the central animal house of Paris Descartes (centre St Pères) as well as by the ethical committee for animal experimentation of Paris Descartes. We have read the article by Drummond (2008) and the experiments described here comply with journal policies and UK regulations.

Slice preparation: Experiments with electrical stimulation of PF were performed on transverse slices 300 µm thick cut from the cerebellum of 17-23 day old Sprague-Dawley rats. In photolysis experiments, sagittal slices 230 µm thick were used. Briefly, rats were killed by decapitation under general anesthesia

following inhalation of the volatile anesthetic isoflurane following the recommendations of the European commission to be used with the Directive 86/609/EEC. The cerebellum was quickly removed and cooled in ice-cold solution. Following removal of the brain stem the tissue was glued to the stage of a vibrotome (Leica VT1200S, Germany). Slices were kept in a vessel bubbled with 95% O₂ / 5% CO₂ at 34C° for the rest of the day or alternatively for 1h and then allowed to cool down to room temperature. These experiments involved the use of 92 animals.

Solutions: Slice preparation and recordings in experiments with electrical stimulation were made in a bicarbonate buffered solution containing in mM: 115 NaCl, 2.5 KCl, 1.3 NaH₂PO₄, 26 NaHCO₃ and 25 glucose. For slicing the solution contained 4 mM MgCl₂ and 0.5 mM CaCl₂ and for recovery 1 mM MgCl₂ and 2 mM CaCl₂. For recording solutions CaCl₂ and MgCl₂ concentrations were 2.5 and 1 mM respectively. For experiments with electrical stimulation the bath was continuously perfused at a rate of 1 to 2 ml/min with solution equilibrated with 95% O₂ / 5% CO₂ to maintain pH at 7.4. Flash photolysis experiments were done in a HEPES buffered saline without perfusion to minimise cage consumption. This solution contained in mM: 132 NaCl, 4 KCl, 2 NaHCO₃, 10 HEPES, 15 glucose and 5 mM sodium pyruvate (see Holmgren et al., 2009), pH 7.3, supplemented with 1 mM MgCl₂ and 2.5 mM CaCl₂. Bicarbonate was included in the HEPES buffered solution to maintain internal pH.

Whole cell patch clamp recordings were made from Purkinje neurons, identified by their size and location at the edge of the molecular and granule cell layers. The internal solution contained in mM: 140 Kgluconate, 10 KCl, 10 HEPES, 0.1 EGTA, 4.6 MgCl₂, 4 ATPNa₂ and 0.4 GTPNa, pH adjusted to 7.3 with KOH and osmolarity to 300 mOsm/kg. When filled with internal solution, recording pipettes had a resistance between 2.5 and 4.5 MΩ. Membrane currents were recorded at a pipette potential of -60 mV (not corrected for junction potential of approximately -12mV pipette - bath). Series resistance was less than 10 MΩ and was 80% compensated. During experiments, the

preparation was visualised on an upright microscope (Olympus BFX51; 60x 0.9 NA water dipping objective).

Parallel fibers were stimulated with a patch pipette positioned at the surface of the molecular layer. Pulses of 100 μ s duration and around 40 V from an isolated stimulator were used. Similar values were used in all experiments to achieve comparable numbers and density of active PF.

Photolysis was with a xenon arc flashlamp (UV2 filter, Rapp Optoelectronic; Hamburg) generating pulses of 0.5-1 ms with wavelength 330-380 nm. Light was coupled to the epifluorescence condenser of the microscope by a liquid light guide and focused to give a uniform field of 200 μ m diameter. Field uniformity was checked with full field CCD images by flashing 6 μ m diameter fluorescent beads and recorded with an EMCCD camera (Andor Ixon, Belfast). Light flashes were at maximal energy and applied at 2 minute intervals. MNI-caged L-glutamate (kindly provided by Drs John Corrie and George Papageorgiou, MRC-NIMR, London, UK) was used at 270 μ M. Cage was added to the bath with mixing and 5 min allowed for equilibration before photolysis. Calibration of photolysis was with small aqueous vesicles suspended in a thin layer of Sylgard resin and containing the caged fluorophore NPE-HPTS (2-nitrophenylethyl ether of pyranine) as described previously (Canepari et al., 2001; Trigo et al., 2009). The conversion of MNI-glutamate relative to NPE-HPTS in this optical arrangement was 4.7:1 and includes a correction for "inner filtering" by the 270 μ M MNI-glutamate in the bath between preparation and objective that was determined in separate measurements of the transmission of the photolysis pulse in the bath.

Chemicals: 2,3-Dioxo-6-nitro-1,2,3,4-tetrahydrobenzo[f]quinoxaline-7-sulfonamide (NBQX), 2-(3-Carboxypropyl)-3-amino-6-(4methoxyphenyl)pyridazinium bromide (SR 95531), D-(-)-2-Amino-5-phosphonopentanoic acid (D-AP5), 7-(Hydroxyiminocyclopropa[b]chromen-1a-carboxylate ethyl ester (CPCCOEt), γ -D-Glutamylglycine (γ -DGG), 7-Chlorokynurenic acid (7-Cl-Kyn), 1-(1,1-Dimethylethyl)-1-(4-methylphenyl)-1H-

pyrazolo[3,4-d]pyrimidin-4-amine (PP1) and TTX were purchased from Tocris Bioscience. Alternatively, SR 95531, CPCCOEt and D-AP5 were bought from Ascent Scientific. bpv(Phen) was purchased from Calbiochem. GYKI 53655 was a kind gift from Dr. Michael Spedding. Stocks of CPCCOEt, PP1 and 7-CI-Kyn were prepared in DMSO and stored at -20°C. All other stocks were prepared in water. Stock solutions were diluted in saline just before use. All other chemicals were purchased from Sigma.

Results:

AMPA receptor activation inhibits the mGluR sEPSC.

Train stimulation of PF (e.g. 10 pulses at 100 Hz) activates a fast AMPA EPSC followed by a slow mGluR EPSC (Batchelor et al., 1994). In a first set of experiments, it was noticed that the mGluR sEPSC was not observed in the absence of antagonists of AMPA/KA receptors. However, it was almost always observed if AMPA/KA-receptors were blocked with the antagonist NBQX before recording.

This is illustrated in Fig.1. PF were stimulated extracellularly in transverse cerebellar slices by a train of 10 stimuli at 100 Hz activating a fast AMPA EPSC. In most experiments, the stimulation was set to 40 V and 100 μ s duration. The position of the pipette was adjusted to elicit an AMPA EPSC of 0.5 nA to 1 nA. Upon bath application of 1 μ M NBQX, the amplitude of the fast EPSC decreased rapidly and a slower synaptic current became visible (Fig. 1A and B). This mGluR1 sEPSC was blocked by addition of the mGluR1 antagonist CPCCOEt (100 μ M) as described previously by Batchelor et al. (1994; with MCPG) and Canepari et al. (2001). The AMPA EPSC was measured at the peak of the first response of the train but as the AMPA and mGluR currents overlap in control conditions, the analysis window for the sEPSC was chosen based on the current kinetics (see Fig.1). Although this procedure permitted a good separation of the currents, in some cases it underestimated the peak of the mGluR sEPSC. With a K⁺ gluconate internal solution and recording at room temperature, the amplitude of the mGluR sEPSC was $-30.9 \text{ pA} \pm 7.7 \text{ pA}$ (N =

28) in control, $-96.7 \text{ pA} \pm 17.8 \text{ pA}$ ($N = 28$) in $1 \text{ } \mu\text{M}$ NBQX and $-29.3 \text{ pA} \pm 7.8 \text{ pA}$ ($N = 18$) following wash of NBQX.

The AMPA EPSC activated by the PF train is large, producing depolarisation of the dendrites. Although AMPARs in Purkinje cells have a very low permeability to Ca^{2+} (Haüsser and Roth, 1997), the depolarisation due to the EPSC may activate Ca^{2+} entry into the dendrites and may thereby result in Ca^{2+} -activated K^+ conductances. This outward current, which could overlap the inward sEPSC and thereby reduce its apparent amplitude, would be prevented by AMPA receptor antagonists. The possibility that an outward current was generated in this way was tested by blocking the sEPSC with CPCCOEt (see Fig.2). The current amplitude was measured in control in the absence of NBQX or after estimating the amplitude of the sEPSC in NBQX and washing out the drug to directly compare amplitudes. Data were not significantly different and were pooled together. On average, the mGluR sEPSC was $-29.9 \text{ pA} \pm 16.2 \text{ pA}$ in control ($N = 12$), $-113.7 \text{ pA} \pm 34.7 \text{ pA}$ in $1 \mu\text{M}$ NBQX ($N = 7$) and $-19.4 \text{ pA} \pm 6.1 \text{ pA}$ after 20 to 25 minutes wash ($N = 7$). The outward current measured at the same time point as the sEPSC in $100 \text{ } \mu\text{M}$ CPCCOEt was $+16.7 \text{ pA} \pm 3.7 \text{ pA}$ ($N = 12$), too small to explain the sEPSC increase produced by blocking AMPARs. Data are summarised in Fig.2C.

Selectivity of the effect of NBQX on the sEPSC.

NBQX is a competitive antagonist of both AMPA and KA receptors. The potentiation of the mGluR sEPSC by NBQX could therefore be mediated by a block of either AMPA or KA receptors. Experiments were performed to study the specificity of the effect.

First, experiments presented above were made with $1 \text{ } \mu\text{M}$ NBQX, blocking on average 96.3% of the AMPA EPSC. Although this is a low concentration for KA receptors (see Bureau et al., 1999), reducing the NBQX concentration to 300 nM , blocking 72.6% of the AMPA EPSC, was also sufficient to increase the amplitude of the mGluR sEPSC. The mGluR sEPSC was -30.2

pA \pm 10.5 pA (N = 3) in control and -88.5 pA \pm 9.7 pA (N = 3) in the presence of 300 nM NBQX. Although NBQX is an AMPA/KA receptor antagonist, the high sensitivity to NBQX suggests that the modulation of the sEPSC is mediated by AMPARs rather than KARs.

Second, the effect of GYKI 53655, a selective non competitive AMPAR antagonist (Paternain et al., 1995) was tested. Fig. 3A shows that inhibition of AMPARs by GYKI 53655 also increased the amplitude of the mGluR sEPSC. Upon application of 5 μ M GYKI 53655, the fEPSC was rapidly inhibited and the mGluR sEPSC amplitude increased. This is seen both on average traces in Fig. 3Aa and b, and in the amplitude plot of Fig. 3Ac. Both effects were reversible upon washout of the drug. The mGluR sEPSC was -25.2 pA \pm 5.6pA in control (N = 24) and -75.3 pA \pm 11.6 pA (N = 24) in 5 μ M GYKI 53655 (see summary in Fig. 3C). Addition of 1 μ M NBQX further depressed the AMPA EPSC but there was no additional effect on the mGluR sEPSC (see Fig. 3C). On average the mGluR sEPSC was -60.1 pA \pm 13.9 pA (N = 7cells) in GYKI 53655 plus 1 μ M NBQX.

We checked that the current potentiated by GYKI 53655 was identified correctly as due to mGluR1. It was blocked by 100 μ M CPCCOEt (N= 5). The mGluR sEPSC was -27.9 pA \pm 7.6 pA in control, -74.9 pA \pm 17.9 pA in GYKI 53655 and +3.4 pA \pm 0.3 pA in GYKI 53655 + CPCCOEt.

Tests were also made with the non specific low affinity glutamate receptor antagonist γ -DGG. γ -DGG at 1 or 2 mM increased the amplitude of the mGluR sEPSC from -30.0 pA \pm 11.5 pA (N = 10) to -72.1 pA \pm 21.3 pA (N = 10) (see Fig. 3C). No further increase of the mGluR sEPSC was seen with addition of 1 μ M NBQX. The mGluR EPSC was -62.2 pA \pm 16.9 pA (N = 10) in NBQX + γ -DGG.

Experiments presented so far were performed in the presence of 10 μ M D-AP5, a specific NMDA receptor antagonist. However, to test whether NMDA receptors might be involved some experiments were performed in the continued presence of 50 μ M D-AP5, an antagonist of the glutamate binding site, and 25 μ M 7-Chlorokynurenic acid (7-Cl-Kyn), an antagonist of the glycine binding site

of NMDA receptor. In Fig. 2B, the amplitude of the mGluR sEPSC was -25 pA in D-AP5 + 7-Cl-Kyn and -99.8 pA after addition of 1 μ M NBQX. On average the mGluR sEPSC was $-50.8 \text{ pA} \pm 13.5 \text{ pA}$ (N=8) in the presence of D-AP5 + 7-Cl-Kyn and $-153.3 \text{ pA} \pm 41.0 \text{ pA}$ (N = 8) after addition of 1 μ M NBQX ($p < 0.02$ Wilcoxon signed Rank Test).

To summarise, the selective inhibition of AMPARs by the non-competitive antagonist GYKI 53655 increased the mGluR sEPSC and occluded the effect of NBQX. Also, NBQX was effective at low concentrations (300 nM – 1 μ M). Together, these observations suggest that the selective inhibition of AMPARs rather than KARs is responsible for the increase of mGluR sEPSC.

Pre- or postsynaptic AMPARs?

In the experiments presented above with PF stimulation, the glutamate released could activate both presynaptic AMPARs, regulating release, and postsynaptic AMPARs, regulating the mGluR pathway in the postsynaptic cell. To study the postsynaptic processes selectively we used flash photolysis of MNI-glutamate to release glutamate independently of presynaptic PFs. Experiments were done in the presence of TTX (1 μ M), gabazine (10 μ M) and D-AP5 (50 μ M). Glutamate was shown to be released uniformly over the whole somatic and dendritic field in a 0.5 to 1 ms flash (see Methods). The results obtained in a representative experiment are shown in Fig. 4. MNI-glutamate was present at a concentration of 270 μ M in HEPES buffered solution without perfusion. In these experiments the temperature was raised to 30°C in order to favor the mGluR pathway and recapture of glutamate by glutamate transporters, two mechanisms with a high temperature dependence. This may help clear the glutamate released in the slice in the absence of perfusion. Under these conditions, stable responses could be elicited in Purkinje cells, with activation of AMPA / KA currents followed by the mGluR current. The mGluR currents observed were much larger than those recorded with PF stimulation because they are evoked in the whole dendritic tree.

Fig. 4A shows the current recorded after release of approximately 70 μM L-glutamate in a 1 ms flash in the absence (control) and in presence of 1 μM or 10 μM NBQX. The amplitude of the early, rapidly decaying current was reduced in 1 μM NBQX due to block of AMPA/KA receptors, and the amplitude of the late current simultaneously increased. The peak of the late current seen in NBQX was sufficiently delayed with respect to the early current that it could be readily distinguished. Fig. 4B shows how the amplitudes of the early NBQX-sensitive AMPA receptor mediated currents and of the late mGluR-mediated currents evolved with time. In this example the amplitude of the mGluR1 mediated current was -0.81 nA in the absence of NBQX. The amplitude increased to -1.62 nA as 1 μM NBQX was applied and declined slightly during the continued presence of 10 μM NBQX. As reported in previous studies (Canepari et al., 2001; Canepari and Ogden, 2003, 2006) the slow component of current evoked by photolytic glutamate release was blocked by the mGluR1 antagonist CPCCOEt (100 μM ; N = 3) and the non-selective group I and II mGluR antagonist RS-MCPG (1mM, N = 5).

On average, the peak slow mGluR1 mediated current was -626 ± 132 pA in control (N=11 cells), -1237 ± 141 pA in 1 μM NBQX (N=11; $P < 0.01$) and -1237 ± 162 pA in 10 μM NBQX (N=8; $P < 0.01$; see Fig.4C). A similar increase was seen with the AMPAR selective antagonist GYKI53655. The mGluR current was $-496 \text{ pA} \pm 95 \text{ pA}$ (N = 7) in control and $-793 \text{ pA} \pm 77 \text{ pA}$ (N = 7) in 5 or 10 μM GYKI 53655. Data are summarised in Fig.4C.

Photolytic glutamate release induced very large AMPA currents in the dendrites of Purkinje cells and gave rise to dendritic calcium spikes. The possibility exists that the amplitude of the mGluR slow current was underestimated because of a Ca^{2+} activated K^+ outward current, arising from dendritic Ca^{2+} influx during the calcium spikes produced by AMPAR activation. This was tested by experiments done in the presence of CPCCOEt. Application of CPCCOEt (100 μM) in the absence of NBQX blocked the mGluR current but did not uncover a contaminating outward K^+ current that might explain the effect of AMPAR inhibition. Furthermore, the photolysis records show that a proportion

of the current attributed to mGluR1 in the absence of AMPAR antagonists is contaminated with a component of AMPAR current, leading to an underestimation of the mGluR1 potentiation attributed to AMPAR block.

The experiments described above with photolytic release of L-glutamate indicate that the facilitation of the mGluR1 current seen with AMPA receptor antagonists at the PF-Purkinje cell synapse is a postsynaptic phenomenon, involving a cross talk between AMPARs and the mGluR signaling pathway.

Inhibition of src-family tyrosine kinases.

Specific inhibitors have previously been used to investigate the signalling pathway initiated by activation of mGluR1 by photolytic glutamate release (Canepari and Ogden, 2003, 2006). These experiments showed that inhibition of protein tyrosine phosphatase inhibited the mGluR1 current and inhibition of tyrosine kinase potentiated submaximal mGluR1 currents. The known selectivity of the most active inhibitory ligands indicated that src-family tyrosine kinase and tyrosine phosphatase are a regulatory pathway. Furthermore, it has been reported that GluR2 AMPAR activation activates an associated Lyn tyrosine kinase by a metabotropic mechanism that does not require channel permeation (Hayashi et al., 2001). Consequently, a src-family PTK inhibitor, PP1, and a protein tyrosine phosphatase inhibitor, bpv(Phen), were used here to test the involvement of tyrosine phosphorylation/dephosphorylation in the regulation of the mGluR1 current by AMPARs in Purkinje cells.

Addition of 10 μM PP1 in the patch pipette produced a potentiation of the sEPSC compared with control recordings. PP1 was dissolved initially in DMSO which was present at a final concentration of 0.1% v/v. This concentration of DMSO was present in interleaved control recordings. With PP1 in the recording pipette, the sEPSC was $-58.45 \text{ pA} \pm 9.4 \text{ pA}$ (N = 9 cells and measured at 20 min WCR). On addition of 1 μM NBQX there was a non significant increase to $-63.3 \text{ pA} \pm 15.1 \text{ pA}$ and subsequently a decline to $-41.8 \text{ pA} \pm 12.5 \text{ pA}$ after 20 min in NBQX (N = 9 cells). In interleaved controls, infusion of 0.1% DMSO alone in the patch pipette had no effect on the initial mGluR sEPSC amplitude

and furthermore the potentiating effect of adding 1 μM NBQX was seen as described earlier (see Fig. 5A, B and E). On average, the mGluR sEPSC was -12.2 pA \pm 5.8 pA in control, -42.1 \pm 11.3 pA in 1 μM NBQX (at the beginning of AMPA block) and -31.0 pA \pm 8.2 pA at 20 min NBQX (N = 7 cells). Figs. 5 A and C present averages of 5 (control) and 9 cells (PP1) over time in whole cell. Two cells were excluded from the control average as they showed no mGluR sEPSC under either set of conditions and could not be included in the normalisation of data.

The potentiation of the mGluR sEPSC by PP1 was apparent very quickly on establishing the whole cell recordings. For this reason the possibility that it was acting externally after ejection from the pipette was tested by applying PP1 extracellularly at 10 μM using a local application pipette or simple bath perfusion. No effect was seen on the mGluR sEPSC. The sEPSC was -11.8 \pm 5.7 pA without PP1 (N = 9), -7.5 \pm 4.2 pA in the presence of external PP1 (N = 11) and -55.9 \pm 23.8 pA in 1 μM NBQX (N = 10) (Fig. 5F). This suggests that PP1 acts intracellularly as it diffuses into the postsynaptic Purkinje cell.

Thus, intracellularly applied tyrosine kinase inhibitor PP1 increased the amplitude of the mGluR sEPSC, mimicking the effect seen when AMPAR were blocked. Furthermore, PP1 also occluded the enhancing effect of NBQX block of AMPAR on the mGluR1 sEPSC. These results suggest that activation of synaptic AMPARs inhibits the mGluR1 sEPSC via the postsynaptic activation of a protein tyrosine kinase. The requirement for postsynaptic intracellular application of PP1 and the ineffectiveness of extracellular application also indicates that PTK signalling from AMPARs to mGluR1 is postsynaptic.

The tyrosine phosphatase inhibitor bpv(Phen) (Posner et al., 1994) applied at 100 μM to the bath inhibited the mGluR sEPSC, as previously reported for photolytically released L-glutamate (Canepari and Ogden, 2003; 2006). Data averaged from 9 cells showed a mGluR sEPSC of -31.1 \pm 7.9 pA in control, -77.6 \pm 14.7 pA in 1 μM NBQX or 10 μM GYKI, and -17.9 \pm 6.2 pA after 10 min in 100 μM bpv(Phen), 20.8 % \pm 5.3 % of the value in NBQX or GYKI (N = 9 cells). The data are given in Fig.S1. The possibility that bpv(Phen)

was acting presynaptically in these experiments was tested. In the absence of AMPAR antagonist the AMPA EPSC was $98.3 \% \pm 7.2 \%$ (N = 4) of the control value after 10 min application of $100\mu\text{M}$ bpv(Phen), indicating that bpv(Phen) did not affect presynaptic release and was acting postsynaptically.

Discussion

We have shown in cerebellar Purkinje cells that AMPAR inhibition facilitates the mGluR1 sEPSC. This regulation does not involve either KA or NMDA receptors, being specific to AMPARs activation. It is also observed when receptors are activated by photorelease of glutamate, indicating that it is a postsynaptic phenomenon. Finally, it is occluded by inhibition of src-family protein tyrosine kinases by PP1 applied intracellularly and blocked by the tyrosine phosphatase inhibitor bpv(Phen). This suggests that AMPARs can regulate the mGluR1 pathway postsynaptically *via* protein tyrosine phosphorylation.

The inhibition of mGluR1 signaling described here can be compared with other reports of synaptically induced mGluR1 regulation. Batchelor and Garthwaite (1997) described a facilitation of the PF sEPSP by CF stimulation. The facilitation lasted for about two minutes and the effect of CF stimulation was mimicked by depolarization sufficient to fire Ca^{2+} spikes or by photorelease of Ca^{2+} from the caged Ca^{2+} chelator NPE-EGTA. This differs from the present observations in enhancement rather than depression of mGluR1 by prior AMPAR activation (with CF in their case), the long duration of the effect, and that the experiments were done with low NBQX concentrations present throughout. In contrast to the results of Batchelor and Garthwaite, a study by Jin et al. (2007) showed a long lasting irreversible depression of the mGluR1 sEPSC following repeated burst stimulation of CF or by strong depolarization (5 s at 0 mV), the latter with NBQX present. The results differ from those reported here in not being observed with PF burst stimulation and were irreversible. The present observations show a different phenomenon, an inhibition of mGluR1 signaling that is prevented by block of AMPA receptors and is readily reversible.

The possible involvement of presynaptic AMPA/KA receptors may also be considered. Presynaptic KA receptors regulate release at PF synapses, facilitating release onto Purkinje cells during bursts (Delaney and Jahr, 2002). In their study Delaney and Jahr (2002) showed that application of NBQX at 10 μ M decreased release. Here we show that low concentrations of NBQX are sufficient to enhance the mGluR sEPSC, and the similar action of the specific AMPAR antagonist GYKI 53655 indicates that the effect here is mediated by AMPARs. Further, we show that it is not a presynaptic effect. It is blocked by postsynaptic infusion of PP1 and seen with direct activation of postsynaptic AMPAR by flash photolysis. The effect of inhibiting postsynaptic AMPARs we describe here and that of inhibiting presynaptic KARs described by Delaney and Jahr (2002) are therefore clearly distinguishable.

The possibility that potentiation by AMPA receptor block might be indirect should be considered. AMPA receptor activation will have produced dendritic depolarization of the dendrites and sub threshold Ca^{2+} entry because of the poor space clamp even in the absence of Ca^{2+} spiking. High intracellular Ca^{2+} has been shown to increase the amplitude of the sEPSC (Batchelor and Garthwaite, 1997; Dzubay and Otis, 2002) and sequestering Ca^{2+} with high intracellular BAPTA concentrations blocks the sEPSC (Dzubay and Otis, 2002; Hildebrandt et al., 2009). Reducing the activation of AMPA receptors is expected to decrease Ca^{2+} entry and therefore the mGluR1 sEPSC by this mechanism, opposite to the observations reported here.

An earlier systematic pharmacological dissection of the coupling of mGluR1 activation to the sEPSC showed evidence of regulation only by protein tyrosine kinase and phosphatase and by G-protein, serine/threonine kinase inhibition showing no effect (Canepari and Ogden, 2003). Evidence of metabotropic actions of AMPA receptors themselves have been shown for the activation of the G-protein G_i (GluR1; Wang et al., 1997) and the activation of the src-family non-receptor PTK Lyn (Hayashi et al., 1999). Lyn was shown to co-precipitate with GluR2 in cerebellar Purkinje cells and to be activated by high

but not by low concentrations of the agonist AMPA (Hayashi et al., 1999). These observations were made in tissue culture, necessitating long exposures to AMPA. Here, in contrast, we have shown that the potentiation of mGluR currents by block of AMPA receptors can be seen with brief exposure to synaptically released L-glutamate. If the effect is mediated by Lyn this indicates that the kinase can be activated by a much shorter activation of AMPA receptors, on the time scale of synaptic transmission. The ability of tyrosine phosphatase inhibition to suppress the sEPSC, the PLC-mediated Ca^{2+} release and the enhancement of T-type Ca-channels suggests that the target of tyrosine phosphorylation is mGluR1 or the G-protein Gq.

The increase in amplitude of the mGluR1 current and the block of the AMPAR current occur in parallel, within the time of the response to each synaptic burst stimulation. No delay was seen in the development of the mGluR current. The inhibitory effect of AMPAR activation therefore takes place before the observed rise of the mGluR sEPSC, i.e. within about 250 ms.

Implications for Ca^{2+} signaling:

mGluR1 receptors in Purkinje cells have been shown to act through three pathways that are influenced by PTK/PTP and which may alter excitability and intracellular Ca^{2+} concentrations. These are, first, the sEPSC described here which is partly carried by Ca^{2+} ions and has been shown to contribute to a slow Ca^{2+} rise (Canepari et al 2004). Second, Ca^{2+} release from intracellular stores mediated by PLC generates a transient Ca^{2+} concentration that activates an inhibitory Ca^{2+} dependent 'BK' K^+ conductance (Canepari and Ogden 2006). Although activated at approximately 2-fold lower L-glutamate concentration than the sEPSC, this pathway additionally requires priming by Ca^{2+} influx in P/Q channels and its contribution may be modified by local activity. Furthermore, it is activated more quickly than the sEPSC, with a delay of 100 ms, and we do not know whether the regulation by AMPA receptors is fast enough in this case. Because of the shorter delay it is difficult to separate the transient K^+ current from the sEPSC in electrical recordings, however this might be achieved with

Ca²⁺ indicators in future experiments. Finally, Hildebrand et al., (2009) have shown that mGluR1 activation potentiates T-type Ca²⁺ channels in Purkinje cells and that this is also potentiated by tyrosine kinase inhibitors. All three PTK/PTP regulated pathways will be expected to result in an increase of intracellular Ca²⁺ on reducing AMPA receptor activation, although the Ca²⁺ release pathway is less predictable because of the requirement for priming by Ca²⁺ influx.

Functional implications:

Glutamate receptor antagonists have been used to better visualise and isolate the mGluR sEPSC. In fact, all studies of the mGluR current using synaptic stimulation that we have found in the literature have been done in the presence of AMPAR antagonists. The present work shows that the mGluR1 pathway is facilitated in these conditions and that we have not fully understood the conditions required for physiological activation of the mGluR1 sEPSC.

Immunogold labelling shows mGluR1 localised at the edge and AMPA receptors centrally at PF-Purkinje cell synapses (Baude et al., 1993). The inhibition of mGluR1 signaling by AMPAR activation will be greatest when the synapse operates with glutamate at high concentration released directly from the presynaptic terminal. On the other hand, if glutamate diffuses from nearby synapses or from ectopic release sites (Matsui and Jahr, 2005), it will reach the mGluR1 first and the AMPARs at a lower concentration. In this configuration the inhibitory cascade would be less active. Thus, the gain of the mGluR1 signal will be set by activation of local AMPARs: it will be high for glutamate diffusing from nearby synapses which encounters first the mGluRs, and low for glutamate released at the same synapse which rapidly activates first the AMPARs. This type of regulation would allow the synapse to distinguish between local or spillover glutamate. Indeed, similar concentrations reached by local release or spillover do not have the same implications for the synapse. Locally, this might correspond to limited release, whereas the same concentration for spillover glutamate might correspond to massive remote synaptic release.

Much evidence shows that mgluR1 are required for motor learning and

for long term depression (LTD) at PF synapses (Aiba et al., 1994; Conguet et al 1994; Coesmans et al., 2003). However, it is less clear that they are essential for the induction of experimental LTD (Biderot et al., 2009). LTD is thought to result from net loss of AMPA receptors by enhanced endocytosis from PF synapses (Wang and Linden, 2000). Once LTD is induced, thereby reducing the postsynaptic activation of AMPARs, mGluR1 signalling will be selectively enhanced. As a potential correlate, Isope and Barbour (2002) showed that in the adult rat, the fraction of silent synapses between PF and Purkinje neuron is very high (approximately 85%). Both at depressed synapses and silent synapses, mGluR1 signalling is expected to be more prominent.

References

- Aiba A, Kano M, Chen C, Stanton ME, Fox GD, Herrup K, Zwingman TA, Tonegawa S (1994) Deficient cerebellar long-term depression and impaired motor learning in mGluR1 mutant mice. *Cell* 79: 377-388.
- Batchelor AM, Garthwaite J (1993) Novel synaptic potentials in cerebellar purkinje cells: probable mediation by metabotropic glutamate receptors. *Neuropharmacology* 32: 11-20.
- Batchelor AM, Garthwaite J (1997) Frequency detection and temporally dispersed synaptic signal associated through a metabotropic glutamate receptor pathway. *Nature* 385: 74-77.
- Batchelor AM, Madge DJ, Garthwaite J (1994) Synaptic activation of metabotropic glutamate receptors in the parallel fibre-Purkinje cell pathway in rat cerebellar slices. *Neuroscience* 63: 911–915.
- Baude A, Nusser Z, Roberts JDB, Mulvihill E, McIlhinney RAJ, Somogyi P (1993) The metabotropic glutamate receptor (mGluR1 alpha) is concentrated at perisynaptic membrane of neuronal subpopulations as detected by immunogoldreaction. *Neuron* 11, 771–787.
- Bidoret C, Ayon A, Barbour B, Casado M. (2009) Presynaptic NR2A-containing NMDA receptors implement a high-pass filter synaptic plasticity rule. *Proc Natl Acad Sci U S A* 106:14126-31.

Brasnjo G, Otis TS (2001) Neuronal glutamate transporters control activation of postsynaptic metabotropic glutamate receptors and influence cerebellar long-term depression. *Neuron* 31, 607–616.

Brunel N, Hakim V, Isope P, Nadal JP, Barbour B (2004) Optimal information storage and the distribution of synaptic weights: perceptron vs Purkinje cell. *Neuron* 43: 745-757.

Bureau I, Bischoff S, Heinemann SF, Mulle C (1999) Kainate receptor-mediated responses in the CA1 field of wild-type and GluR6-deficient mice. *J Neurosci* 19: 653-663.

Canepari M, Auger C, Ogden D (2004) Ca^{2+} ion permeability and single-channel properties of the metabotropic slow EPSC of rat Purkinje neurons. *J Neurosci* 24: 3563-3573.

Canepari M, Papageorgiou G, Corrie JET, Watkins C, Ogden D (2001) The conductance underlying the parallel fibre slow EPSP in rat cerebellar Purkinje neurones studied with photolytic release of L-glutamate. *J Physiol* 533, 765–772.

Canepari M, Ogden D (2003) Evidence for protein tyrosine phosphatase, tyrosine kinase, and G-protein regulation of the parallel fiber metabotropic slow EPSC of rat cerebellar Purkinje neurons. *J Neurosci* 23: 4066–4071.

Canepari M, Ogden D (2006) Kinetic, pharmacological and activity-dependent separation of two Ca^{2+} signalling pathways mediated by type 1 metabotropic glutamate receptors in rat Purkinje neurones. *J Physiol* 573: 65-82.

Coesmans M, Smitt PA, Linden DJ, Shigemoto R, Hirano T, Yamakawa Y, van Alphen, AM, Luo C, van der Geest JN, Kros JM, Gaillard CA, Frens MA, de Zeeuw CI. (2003) Mechanisms underlying cerebellar motor deficits due to mGluR1-autoantibodies. *Ann Neurol.* 53(3):325-36.

Conquet F, Bashir ZI, Davies CH, Daniel H, Ferraguti F, Bordi F, Franz-Bacon K, Reggiani A, Matarese V, Condé F, Collingridge GL, Crépel F (1994) Motor deficit and impairment of synaptic plasticity in mice lacking mGluR1. *Nature* 372:237-43.

Delaney AJ, Jahr CE (2002) Kainate receptors differentially regulate release at

two parallel fiber synapses. *Neuron* 36: 475-482.

Drummond GB (2008) Reporting ethical matters in *The Journal of Physiology*. *J Physiol* 587, 713-719.

Dzubay JA, Otis TS (2002) Climbing fiber action of metabotropic glutamate receptors on cerebellar Purkinje neurons. *Neuron* 36: 1159-1167.

Galante M, Diana M (2004) Group I metabotropic glutamate receptors inhibit GABA release at interneuron-purkinje cell synapses through endocannabinoid production. *J Neurosci* 24: 4865-4874.

Hartmann J, Blum R, Kovalchuk Y, Adelsberger H, Kuner R, Durand GM, Miyata M, Kano M, Offermanns S, Konnerth A (2004) Distinct roles of $G\alpha_q$ and $G11$ for Purkinje cell signalling and motor behavior. *J Neurosci* 24: 5119–5130.

Hartmann J, Dragicevic E, Adelsberger H, Henning HA, Sumser M, Abramowitz J, Blum R, Dietrich A, Freichel M, Flockerzi V, Birnbaumer L, Konnerth A (2008) TRPC3 Channels Are Required for Synaptic Transmission and Motor Coordination. *Neuron* 59, 392–398.

Häusser M, Roth A (1997) Dendritic and somatic glutamate receptor channels in rat cerebellar Purkinje cells. *J Physiol* 501: 77-95.

Hayashi T, Umemori H, Mishina M, Yamamoto T (1999) The AMPA receptor interacts with and signals through the protein tyrosine kinase Lyn. *Nature* 397: 72-76.

Hildebrand ME, Isope P, Miyazaki T, Nakaya T, Garcia E, Feltz A, Schneider T, Hescheler J, Kano M, Sakimura K, Watanabe M, Dieudonné S, Snutch TP (2009) Functional coupling between mgluR1 and Cav3.1 T-type calcium channels contributes to parallel fibre-induced fast calcium signaling within Purkinje cells dendritic spines. *J Neurosci* 29: 9668-9682.

Hirono M, Konishi S, Yoshioka T (1998) Phospholipase C-independent group I metabotropic glutamate receptor-mediated inward current in mouse Purkinje cells. *Biochem Biophys Res Commun* 251:753–758.

Holmgren CD, Mukhtarov M, Rheims S, Malkov AE, Popova IY, Khalilov I, Zilberter T, Bregestovski P, Zilberter Y (2009) Energy substrate availability as a

determinant of neuronal resting potential, GABA signaling and spontaneous network activity in the neonatal cortex. *J Neurochem* 112, 900-912.

Isope P, Barbour B (2002) Properties of unitary granule cell → Purkinje cell synapses in adult rat cerebellar slices. *J Neurosci* 22: 9668-9678.

Jin Y, Kim SJ, Kim J, Worley PF, Linden DJ (2007) Long-term depression of mGluR1 signalling. *Neuron* 55: 277-287.

Kim SJ, Kim YS, Yuan JP, Petralia RS, Worley PF, Linden DJ (2003) Activation of the TRPC1 cation channel by metabotropic glutamate receptor mGluR1. *Nature* 426: 285-291.

Maejima T, Oka S, Hashimoto-dani Y, Ohno-Shosaku T, Aiba A, Wu D, Waku K, Sugiura T, Kano M (2005) Synaptically driven endocannabinoid release requires Ca²⁺-assisted metabotropic glutamate receptor subtype 1 to phospholipase C β 4 signalling cascade in the cerebellum. *J Neurosci* 25: 6826-6835.

Marcaggi P, Attwell D (2005) Endocannabinoid signalling depends on the spatial pattern of synapse activation. *Nat Neurosci* 8:1-6.

Matsui K, Jahr CE (2005) Ectopic release of synaptic vesicles. *Neuron* 40: 1173-1183.

Nusser Z, Mulvihill E, Streit P, Somogyi P (1994) Subsynaptic segregation of metabotropic and ionotropic glutamate receptors as revealed by immunogold localization. *Neuroscience* 61: 421-427.

Paternain AV, Morales M, Lerma J (1995) Selective antagonism of AMPA receptors unmasks Kainate receptors-mediated responses in hippocampal neurons. *Neuron* 14: 185-189.

Petralia RS, Zhao H-M, Wang Y-X, Wenthold RJ (1998) Variations in the tangential distribution of postsynaptic glutamate receptors in Purkinje cells parallel and climbing fiber synapses during development. *Neuropharmacology* 37: 1321-1334.

Posner BI, Faure R, Burgess JW, Bevan AP, Lachance D, Zhang-Sun G, Fantus G, Ng JB, Hall DA, Lum BS, Shaver A (1994) Peroxovanadium compounds. *J Biol Chem* 269: 4596-4604.

Reichelt W, Knopfel T (2002) Glutamate uptake controls the expression of a

slow postsynaptic current mediated by mGluRs in cerebellar Purkinje cells. *J Neurophysiol* 87: 1974-1980.

Tempia F, Alojado ME, Strata P, Knopfel T (2001) Characterisation of the mGluR1-mediated electrical and calcium signaling in Purkinje cells of the mouse cerebellar slices. *J Neurophysiol* 86: 1389-1397.

Tempia F, Miniaci M C, Anchisi D, Strata P (1998) Postsynaptic current mediated by metabotropic glutamate receptors in cerebellar Purkinje cells. *J Neurophysiol* 80: 520–528.

Trigo FF, Corrie JE, Ogden D (2009) Laser photolysis of caged compounds at 405nm: photochemical advantages, localisation, phototoxicity and methods for calibration. *J Neurosci Methods* 180: 9-21.

Wadiche JI, Jahr CE (2005) Patterned expression of Purkinje cell glutamate transporters controls synaptic plasticity. *Nat neurosci* 8: 1329-1334.

Wang Y, Small DL, Stanimirovic DB, Morley P, Durkin JP (1997) AMPA receptor-mediated regulation of a G_i-protein in cortical neurons. *Nature* 389: 502-504.

Wang YT, Linden DJ (2000) Expression of cerebellar long-term depression requires postsynaptic clathrin-mediated endocytosis. *Neuron* 25:635-47.

Author contributions: Both authors contributed to the conception and design of the experiments, drafting and revising the article and approved the final version to be published. Analysis and interpretation of the data were done by C. Auger. The whole study was performed at the Laboratoire de Physiologie cérébrale, Université Paris Descartes.

Acknowledgements: We thank Alain Marty, Isabel Llano, Jacsue Kehoe and Philippe Ascher for discussion and comments on the manuscript. This work was supported by the Centre National de la Recherche Scientifique, the Agence Nationale pour la Recherche, the Fondation pour la Recherche Médicale, and EU (PHOTOLYSIS -LSHM-CT-2007-037765).

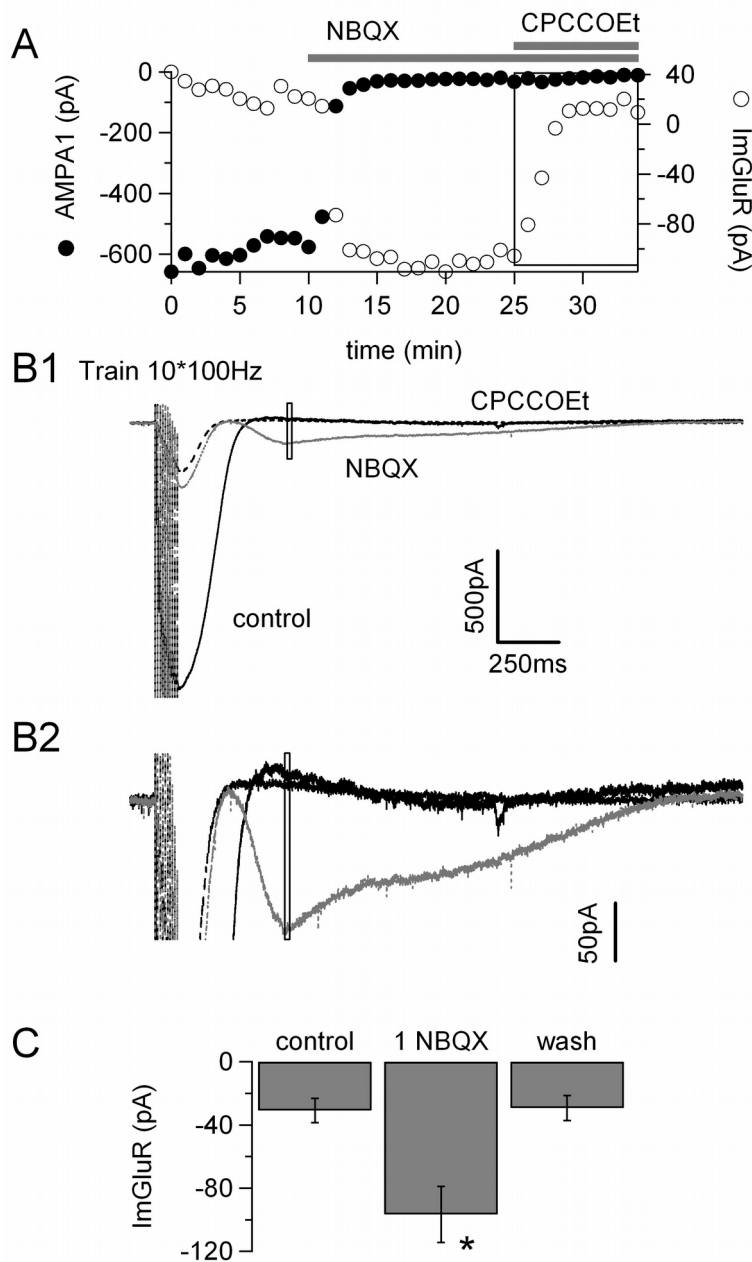


Figure 1 : The mGluR1 sEPSC is enhanced by inhibition of AMPA/KARs.

A, plot of the amplitude of the first AMPA response of the train (AMPA1, filled symbols) and mGluR sEPSC (open symbols) as a function of time. Bars indicate time of application. B, average of 4 (control) or 5 (NBQX and CPCCOEt) postsynaptic responses to burst stimulation of parallel fibers (10 at 100 Hz) in a transverse slice. B1, black trace in control, dotted grey trace after

addition of 1 μM NBQX and dotted black trace after further addition of 100 μM CPCCOEt. In the presence of NBQX the fast AMPA current is quickly blocked and the mGluR sEPSC becomes visible. Upon application of CPCCOEt the mGluR sEPSC is fully blocked. The empty rectangle denotes the time window used to measure the average amplitude of ImGluR plotted in A. B2, same traces at higher magnification to emphasize the mGluR sEPSC. C, average mGluR sEPSC \pm sem (* data significantly different from control $p < 0.01$).

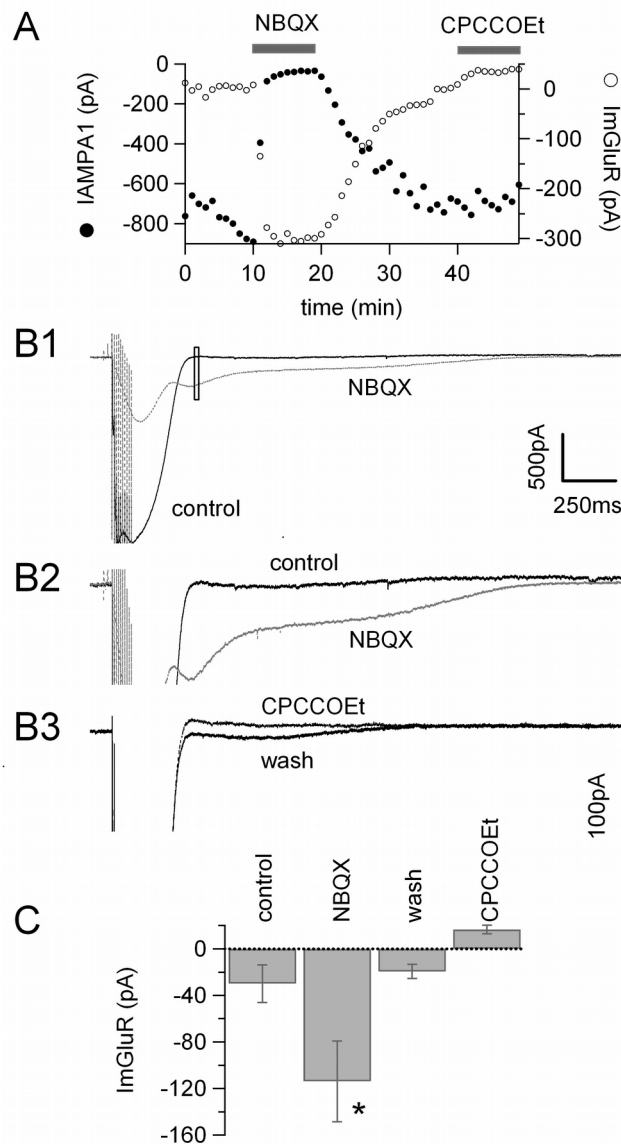


Figure 2 : Overlap with a K⁺ conductance does not explain the reduced amplitude of the mGluR sEPSC in control conditions. A, plot of the amplitude of the first AMPA response of the train (AMPA1, filled symbols) and mGluR sEPSC (open symbols) as a function of time. Bars indicate time of application. B, average of 4 (control) or 5 postsynaptic responses to burst stimulation of parallel fibres (10 at 100Hz) in a transverse slice. B1, black trace in control, dotted grey trace after addition of 1 μ M NBQX and dotted black trace after addition of 100 μ M CPCCOEt. In the presence of NBQX the fast AMPA EPSC is quickly blocked and the mGluR sEPSC becomes visible. 1 μ M NBQX

increased the amplitude of the mGluR sEPSC from +2.7pA to -301.7pA. This effect was reversed upon 20 minutes washout of the drug and the mGluR sEPSC measured at the same time point was -6.3pA. Therefore, the wash should have restored the K⁺ outward current if it is the source of the apparent inhibition of the mGluR sEPSC. Upon inhibition of mGluR1 by 100μM CPCCOEt, the train activated an outward current of +36.9pA. This outward current however, is not sufficient to account for the decrease of the mGluR sEPSC during wash of NBQX. The empty rectangle denotes the time window used to measure the amplitude of ImGluR plotted in A. B2, same traces at higher magnification to emphasize the mGluR sEPSC. C, average mGluR sEPSC ± sem (* data significantly different from control p< 0.02).

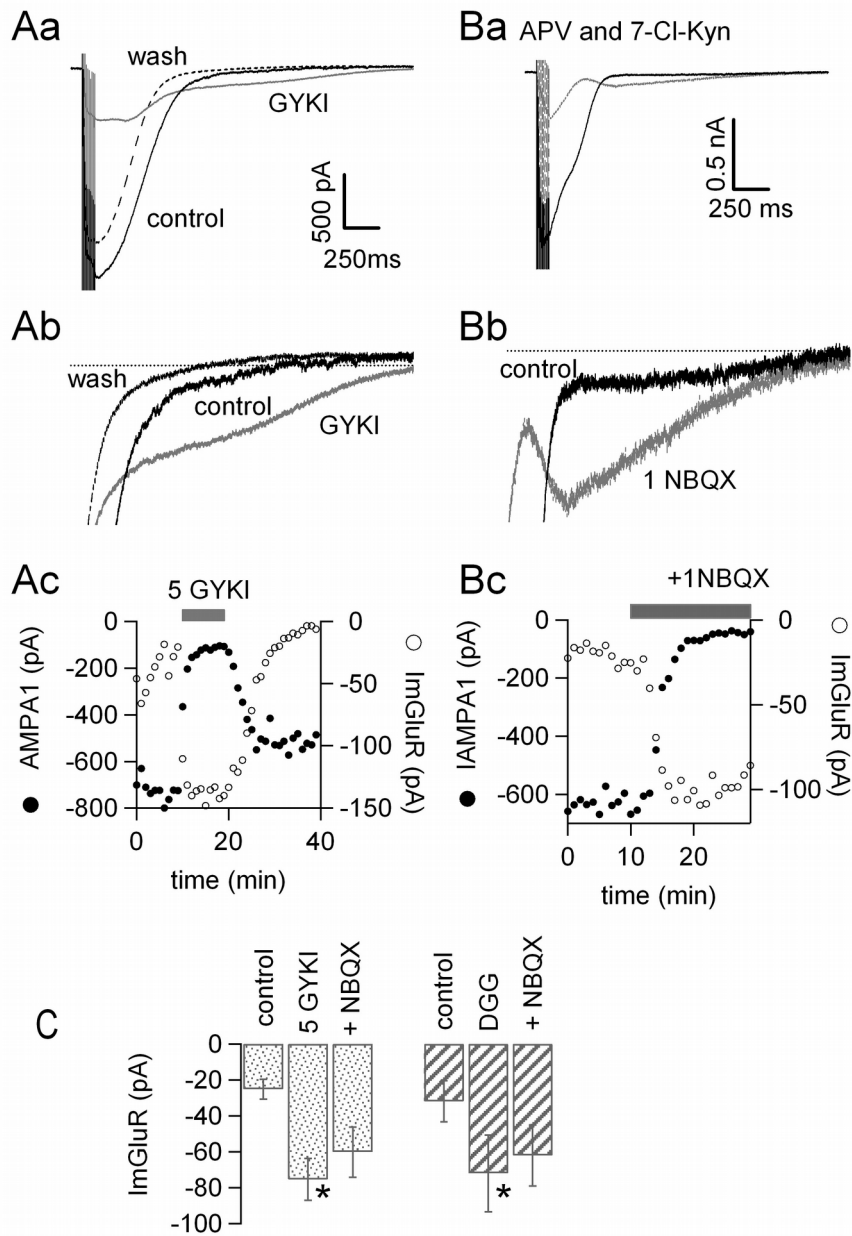


Figure 3 : Selective inhibition of AMPARs enhances mGluR sEPSC.

Aa, average postsynaptic currents following burst stimulation (10 at 100Hz) in control (average of 3 traces, black), GYKI53655 5 μ M (average of 5 traces, grey) and wash (average of 5 traces, dotted line). Ab, same but at higher magnification to emphasize the mGluR sEPSC. GYKI increased the mGluR sEPSC reversibly. Ac, amplitude plot of the first AMPA response in the train (AMPA1, filled symbols) and the mGluR sEPSC (open symbols). Ba and Bb,

average postsynaptic currents following 10 stimulations at 100 Hz in control (average of 4 traces) and 1 μ M NBQX (average of 5 traces) in the continued presence of 50 μ M D-AP5 and 25 μ M 7-Cl-Kyn. Block of NMDARs does not affect the potentiation of mGluR sEPSC by NBQX. Bc, amplitude plot of the first AMPA response (filled symbols) in the train and the mGluR sEPSC (open symbols) in the presence of 50 μ M D-AP5 and 25 μ M 7-Cl-Kyn. Bars indicate application time. C, bar graph of the average amplitude \pm sem of mGluR sEPSC. (* data significantly different from control $p < 0.01$).

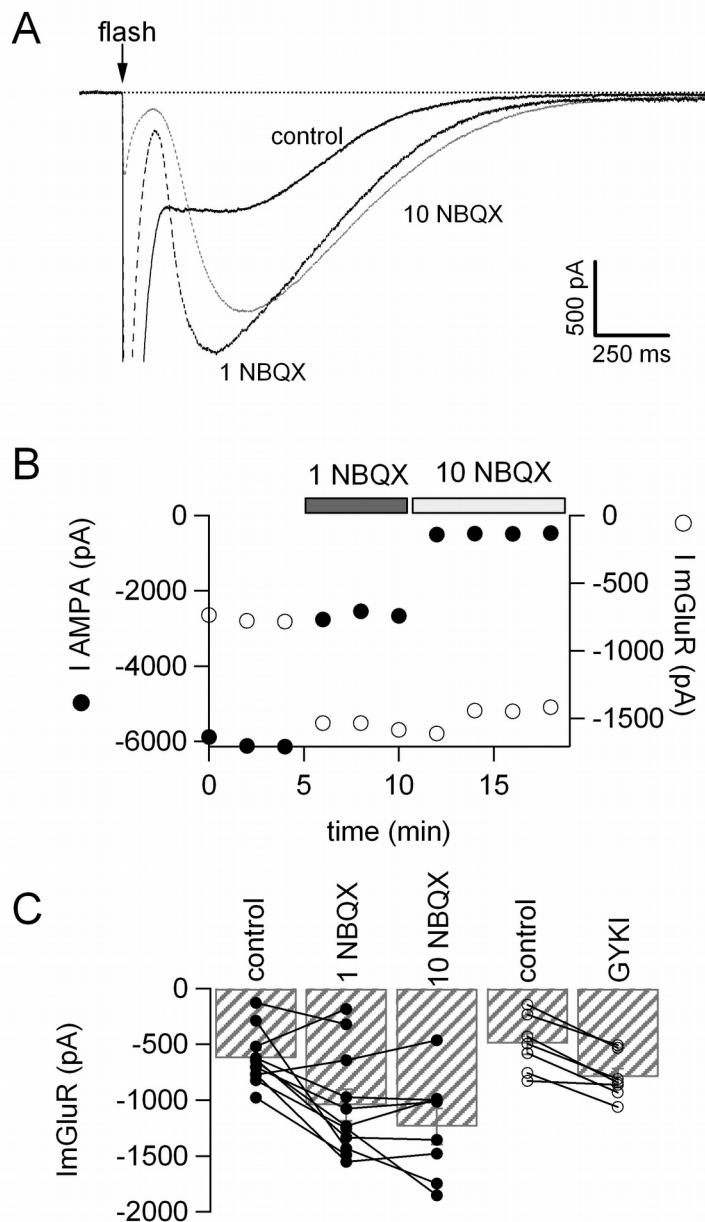


Figure 4 : The mGluR current elicited by flash photolysis of glutamate is also facilitated by AMPAR inhibition. A, flash photolysis of MNI-glutamate at the time indicated by the arrow activated a fast AMPA/KA current and a slow mGluR current (control trace in black, average of 3 traces). Upon partial block of the AMPA response by 1 μM NBQX (dotted black trace, average of 3 traces) the peak mGluR current increased from -807 pA to -1624 pA. Further block of the AMPA current following addition of 10 μM NBQX (dotted grey trace, average of 4

traces) failed to potentiate the mgluR amplitude further. B, amplitude plot of the AMPA/KA current and mGluR current. C, bar graph of the average amplitude \pm sem for the mGluR current and individual data points. Both NBQX and GYKI increased the amplitude of the current significantly (Wilcoxon signed Ranked test, $p < 0.01$ and $p < 0.02$ respectively).

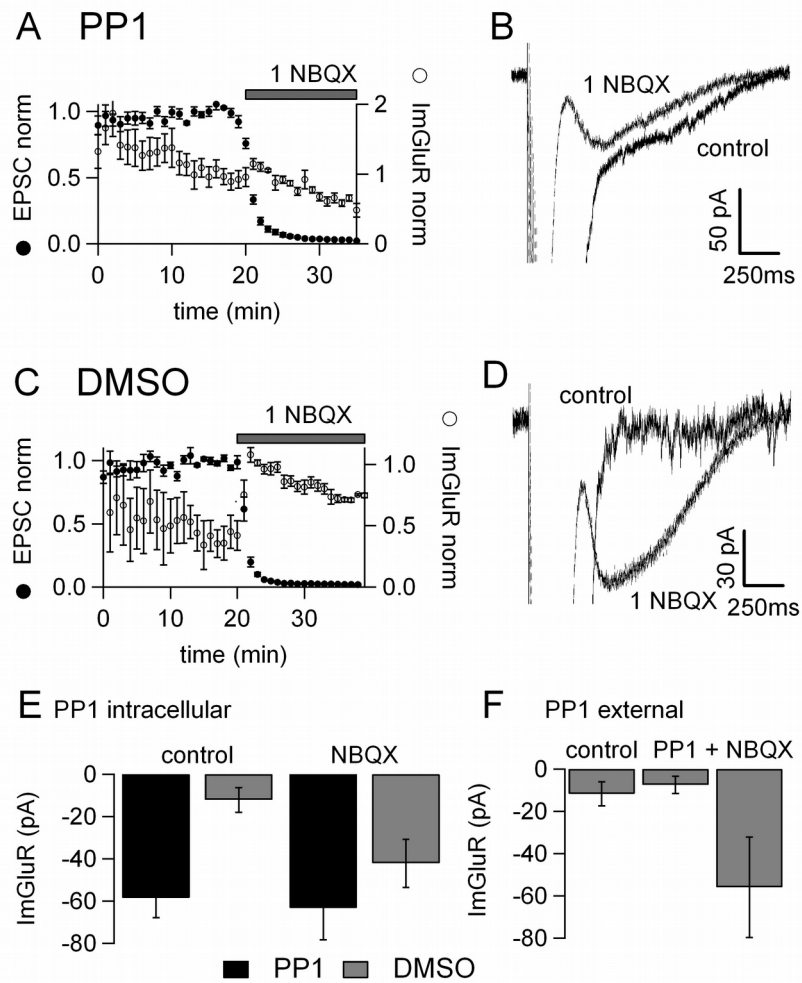


Figure 5 : The src-family tyrosine kinase inhibitor PP1 occludes the effect of AMPAR inhibition. A and B, 10 μ M PP1 (+0.1% DMSO) was added to the internal solution and allowed to diffuse for 20 min into the postsynaptic Purkinje cell via the patch pipette. C and D, interleaved control experiments with 0.1% DMSO added to the internal solution. A and C, average amplitude plot of AMPA fEPSC and mGluR sEPSC normalised to the response at the beginning of AMPA block. A, there is no significant increase of the sEPSC amplitude following NBQX application. C, with DMSO only, there is a large increase of the mGluR sEPSC with respect to control. B and D show average traces with no significant increase when PP1 is infused into the cell and a large increase for the DMSO only experiment. E, bar graph of average amplitude \pm sem of mGluR sEPSC for cells recorded with PP1 supplemented internal (black) and control

with DMSO (grey). Control values were taken at 20 min whole cell recording and NBQX values at the peak of the effect. With PP1 the control value was increased and there was no further effect of NBQX whereas in control interleaved recordings, there was a potentiation of the sEPSC. PP1 was different from DMSO control $p < 0.01$. Control and NBQX were statistically different for DMSO experiments ($p < 0.05$) but not for PP1 experiments. F, bar graph of average amplitude \pm sem of mGluR sEPSC in control, during extracellular application of 10 μ M PP1 and addition of 1 μ M NBQX. Extracellular application of PP1 had no effect on the sEPSC.